International Journal of Pharmaceutics 494 (2015) 417–429

Contents lists available at ScienceDirect

International Journal of Pharmaceutics

journal homepage: www.elsevier.com/locate/ijpharm

A novel scalable manufacturing process for the production of hydrogel-forming microneedle arrays

Rebecca E.M. Lutton, Eneko Larrañeta, Mary-Carmel Kearney, Peter Boyd, A.David Woolfson, Ryan F. Donnelly*

School of Pharmacy, Queens University Belfast, 97 Lisburn Road, Belfast BT9 7BL, United Kingdom

ARTICLE INFO

Article history:
Received 2 July 2015
Received in revised form 14 August 2015
Accepted 17 August 2015
Available online 21 August 2015

Keywords:
Microneedle
Scalable
Manufacture
Injection moulding
Drug delivery
Commercialisation

ABSTRACT

A novel manufacturing process for fabricating microneedle arrays (MN) has been designed and evaluated. The prototype is able to successfully produce 14 × 14 MN arrays and is easily capable of scale-up, enabling the transition from laboratory to industry and subsequent commercialisation. The method requires the custom design of metal MN master templates to produce silicone MN moulds using an injection moulding process. The MN arrays produced using this novel method was compared with centrifugation, the traditional method of producing aqueous hydrogel-forming MN arrays. The results proved that there was negligible difference between either methods, with each producing MN arrays with comparable quality. Both types of MN arrays can be successfully inserted in a skin simulant. In both cases the insertion depth was approximately 60% of the needle length and the height reduction after insertion was in both cases approximately 3%.

© 2015 Elsevier B.V. All rights reserved.

1. Introduction

Microneedle arrays (MN) are minimally-invasive devices that painlessly by-pass the *stratum corneum*, the principal skin barrier to topically-applied drugs, and as such are intended for drug delivery and biosensing (Donnelly et al., 2012; Singh et al., 2010a, b). They consist of a plurality of micro-projections, generally ranging from 25 to 2000 μm in height, which are attached to a base support (Donnelly et al., 2010a,b; Gittard et al., 2013). They have been extensively investigated in recent years as a means to enhance transdermal drug and vaccine delivery with a multitude of fabrication techniques, materials and geometries employed.

Different groups have investigated various types of micro-needles, from in-plane (Paik et al., 2004) and out-of-plane (Donnelly et al., 2010a,b), to hollow (Gardeniers et al., 2003), solid (Ling Teo et al., 2005), macroporous (Ji et al., 2006), dissolving (Donnelly et al., 2013; Migalska et al., 2011) and swelling (Donnelly et al., 2014a; Larrañeta et al., 2015). They have been produced from a variety of materials such as glass (Martanto et al., 2006), sugar (Martin et al., 2012), metal (Martanto et al., 2004), metal coated (Zhu et al., 2012), silicon (Ji et al., 2006), solid polymer (Trautmann et al., 2005), aqueous hydrogel (Donnelly et al., 2014a) and dissolving polymers (Donnelly et al., 2013). Additionally, MN can be prepared using a wide variety of geometries, having a great impact on their performance (Gomaa et al., 2010; Olatunji et al., 2013).

As a result of the range of materials chosen and the variety of shapes designed, MN have been fabricated using a diversity of techniques, mostly from microelectromechanical systems (MEMS) technology. Fabrication techniques range from ion sputtering deposition (Tsuchiya et al., 2010), photolithography (Kochhar et al., 2013), wet and dry etching (Ji et al., 2006), photopolymerisation (Cruise et al., 1998), laser ablation and micromoulding (Aoyagi et al., 2007; Donnelly et al., 2011), layer-by-layer deposition (DeMuth et al., 2013), droplet-born air blowing (Kim et al., 2013), drawing lithography (Lee and Jung 2012) and milling (Yung et al., 2012). Yet, despite the relative degree of success in MN fabrication, there are still very few MN products on the market, in part due to the difficulty in scale-up of fabrication.

Our research group showed the ability of MN to deliver different types of molecules successfully across the skin (Donnelly et al., 2011, 2009, 2014a; Migalska et al., 2011). Recently, our work has focused on designing a MN manufacturing process capable of facile scale-up, taking account of universal acceptance criteria and GMP specifications in moving towards commercialisation (Lutton et al., 2015). A MN insertion quality control test, which could be used during manufacture, has also been developed (Larrañeta et al.,

* Corresponding author at: Chair in Pharmaceutical Technology, School of Pharmacy, Queens University Belfast, Medical Biology Centre, 97 Lisburn Road, Belfast, BT9 7BL, UK. Fax: +44 0 28 90 247 794.
E-mail address: r.donnelly@qub.ac.uk (R.F. Donnelly).

http://dx.doi.org/10.1016/j.ijpharm.2015.08.049
0378-5173/© 2015 Elsevier B.V. All rights reserved.

2014). In addition, research on alternative crosslinking techniques suitable for MN scale-up was conducted reducing 30-fold the crosslinking time (Larrañeta et al., 2015). Currently we produce MN arrays prepared from polymeric materials under ambient conditions in a discrete manner using an excimer laser-based method for micromoulding (Donnelly et al., 2011).

The laser machining process uses a focused optical light beam to selectively remove materials from a substrate to create a desired feature on, or internal to, the substrate. The process is non-contact, yet it has high spatial confinement. Compared to other mechanical machining techniques, laser machining, being a non-contact process, does not incur tool wear and also exhibits low heat deposition to the working piece (Brookhaven National Laboratory, 2013; Sato et al., 2014). However, laser cutting is associated with thermal effects at the cutting surface, resulting in alteration of microstructure and mechanical properties (LaserFocusWorld, 2007; Sato et al., 2014; Zaied et al., 2013). This alterations of microstructure are often associated with undesirable effects such as surface cracking, fatigue resistance and creation of microcracks in the surrounding material. In subsequent routine use of the work piece, these cracks may propagate deep into the bulk of the material and cause premature device failure (Crowson, 2006; Huang et al., 2014; LaserFocusWorld, 2007; Stavinoha, 2001; Zaied et al., 2013). Therefore, in this work we propose the use of injection moulding for the production of MN moulds. Therefore the laser process is not ideal for MN moulds production for larger scale processes.

In the present study, we describe a novel, scalable method of MN manufacture. This method is used to produce MN arrays also from polymeric materials under ambient conditions utilising a combination of injection moulding and roller casting.

2. Materials and methods

2.1. Materials

Gantrez® S-97 (M_w = 1.2 × 10^6), a copolymer obtained from the free acid of methyl vinyl ether and maleic anhydride polymers, was provided by Ashland (Tadworth, Surrey, UK). Poly(ethyleneglycol) (PEG) 10,000 Da was obtained from Sigma–Aldrich (Poole, Dorset, UK). Parafilm®, a flexible thermoplastic sheet (127 mm thickness) made of olefin-type material, was used as skin simulant for insertion studies and was obtained from BRAND GMBH (Wertheim, Germany). Micra-Sil® antimicrobial silicone sheet was purchased from J-Flex (Nottinghamshire UK), MED-4870, MED-4830 and DDR-4320 liquid silicone rubber were all purchased from Nusil Technology (Buckinghamshire, UK), MED-4900-5 yellow dye from Polymer Systems Technology Limited (Buckinghamshire, UK), Dow Corning Silastic® S RTV silicone rubber base and green curing agent from Thompson Bros. Ltd (Newcastle Upon Tyne, UK). Stainless steel and aluminium was sourced from Impact Ireland Metals Ltd. (Newtownabbey, UK) whilst poly(tetrafluoroethylene) (PTFE) was obtained from RS Components Ltd. (Northants, UK).

2.2. Manufacture of roller system

Fig. 1 illustrates the computer-aided design (CAD) images (Solid Edge, Siemens PLC) of the designed device alongside an image of the finished device itself. Three rectangular sections, each 20 mm thick, were machined from a single sheet of stainless steel. Two sections were cut to dimensions 70 mm × 230 mm. These pieces form the lateral walls of the system (Fig. 1A). The third section was machined to 80 mm × 230 mm and formed the base (Fig. 1A). A rectangular slot of dimensions 202 mm x 8 mm was machined through both side walls in order to allow, the roller handle, an 8 mm stainless steel rod, to slide along the device. The three stainless steel sections were then bolted together to form a U-shaped housing (Fig. 1A, B and C).

A PTFE rod (14 mm thick and 23.2 mm in diameter) was used as the roller for the device (Fig. 1B). PTFE was chosen due to its hydrophobicity and anti-adherent properties. An 8 mm hole was placed through the centre for the handle to be inserted.

A roller base plate and frame, each 40 mm × 230 mm, were machined out of 5 mm thick stainless steel plates (Fig. 1A). The base plate was used to house the moulds and as such a 20 mm × 190 mm × 2 mm recess, with 3 mm radius at each corner, was machined along its centre. An additional recess of 14 mm × 12 mm × 1 mm was then machined at either end of the mould recess to act as the home position for the roller. The frame is used to secure the moulds in place during operation and to prevent leakage of the applied formulation. A rectangular section 14 mm × 214 mm was cut out of the frame plate to allow the roller to move along the housing. Eight M4 holes were drilled through both roller frame and the base plate; this was to enable the frame to be fastened to the plate. A further two M2.5 holes were drilled into each end of the roller frame, base plate and housing, to enable the assembled roller frame, moulds and base plate to be secured to the housing during operation. The eight M4 and two M2.5 holes were widened to counterbores of diameter 6 mm and 5 mm, respectively on the roller frame in order to prevent impeding the roller handle whilst in operation. Furthermore, the two additional holes at either end of the parts not only allowed the fixed placement of the mould assembly during operation but also the consistent and accurate alignment of the roller This also facilitated easy removal of the

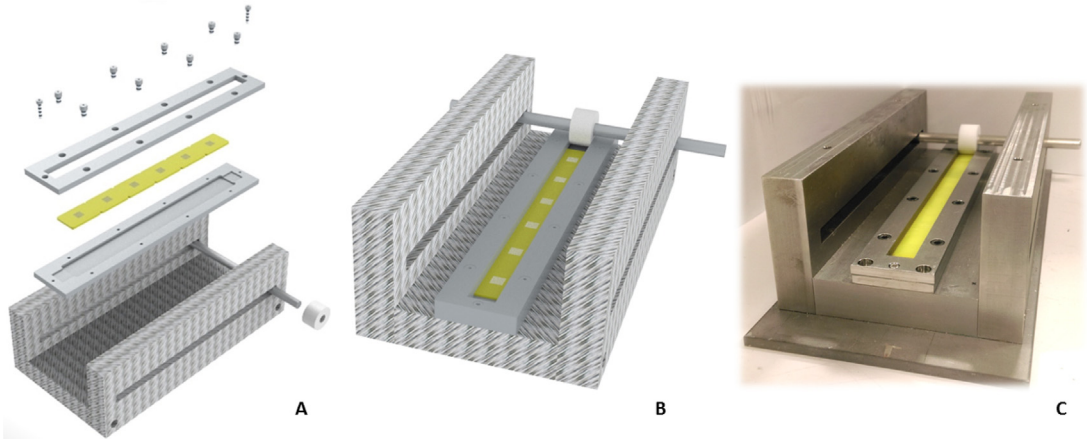

Fig. 1. Exploded CAD image of the roller design (A) CAD image of the roller assembly (B) CAD image of the assembled roller device (C) actual assembled device.

Download English Version:

https://daneshyari.com/en/article/5817964

Download Persian Version:

https://daneshyari.com/article/5817964

Daneshyari.com